

# Dominance of organic aerosols in the marine boundary layer over the Gulf of Maine during NEAQS 2002 and their role in aerosol light scattering

T. S. Bates,<sup>1</sup> P. K. Quinn,<sup>1</sup> D. J. Coffman,<sup>1</sup> and J. E. Johnson<sup>1</sup>

Pacific Marine Environmental Laboratory, NOAA, Seattle, Washington, USA

A. M. Middlebrook

Aeronomy Laboratory, NOAA, Boulder, Colorado, USA

Received 24 January 2005; revised 13 June 2005; accepted 11 July 2005; published 20 September 2005.

[1] Aerosol chemical, physical, and optical measurements were made aboard the NOAA R/V *Ronald H. Brown* off the coast of New England from July 12 through August 10, 2002, as part of the New England Air Quality Study (NEAQS). Measurements (generally 20 to 100 km from the coast) were made downwind of urban centers (New York City, Boston) and rural areas, and in air masses that had not been in contact with land for several days. On average during NEAQS,  $75 \pm 8\%$  of the sub-10  $\mu\text{m}$  aerodynamic diameter dry aerosol mass sampled 18 m above the sea surface was in the sub-1  $\mu\text{m}$  fraction (size cut at 55% RH). The major submicrometer aerosol components were ammonium sulfate and particulate organic matter (POM, defined here as 1.6 times the mass concentration of organic carbon) comprising more than  $92 \pm 4\%$  of the total mass. Under northwesterly flow with an average submicrometer total mass concentrations of  $11 \pm 4.5 \mu\text{g m}^{-3}$ , POM was the dominant component ( $68 \pm 8\%$ ) followed by  $(\text{NH}_4)_x\text{H}_y\text{SO}_4$  ( $23 \pm 8\%$ ), inorganic oxidized material (IOM) ( $6 \pm 4\%$ ), and EC ( $3 \pm 1\%$ ). Under southwesterly flow with an average submicrometer total mass concentrations of  $30 \pm 11 \mu\text{g m}^{-3}$ ,  $(\text{NH}_4)_x\text{H}_y\text{SO}_4$  was the dominant component ( $54 \pm 9\%$ ) followed by POM ( $41 \pm 9\%$ ), IOM ( $3 \pm 2\%$ ), and EC ( $2 \pm 1\%$ ). Mie calculations using submicrometer nonrefractory (NR) POM and NR  $(\text{NH}_4)_x\text{H}_y\text{SO}_4 + \text{H}_2\text{O}$  size distributions to calculate submicrometer light scattering ( $\sigma_{\text{sp}}$ ) at a wavelength of 550 nm suggest that POM was a dominant chemical component contributing to aerosol light scattering (haze) during NEAQS 2002, and contributed  $60 \pm 6\%$  and  $57 \pm 11\%$  to  $\sigma_{\text{sp}}$  at 55% RH during two pollution episodes off the New England Coast. These results are similar to those from the mid-Atlantic states during TARFOX but contrary to the long-term monitoring measurements over the continental northeast United States that show the New England haze is primarily a result of sulfate aerosol.

**Citation:** Bates, T. S., P. K. Quinn, D. J. Coffman, J. E. Johnson, and A. M. Middlebrook (2005), Dominance of organic aerosols in the marine boundary layer over the Gulf of Maine during NEAQS 2002 and their role in aerosol light scattering, *J. Geophys. Res.*, *110*, D18202, doi:10.1029/2005JD005797.

## 1. Introduction

[2] Particles are emitted directly into the atmosphere (e.g., soot, sea salt, crustal material) or are formed in the atmosphere from gas phase precursors such as  $\text{SO}_2$ , volatile organic compounds, ammonia and nitrogen oxides. These particles impair visibility, have the potential to be harmful to human health [Harrison and Yin, 2000], and upon deposition can harm sensitive aquatic and terrestrial

ecosystems [Schindler *et al.*, 1989]. Atmospheric particles also affect the Earth's radiation balance and thus affect climate [IPCC, 2001]. Legislation and regulatory mandates during the past 15 years have reduced  $\text{SO}_2$  and VOC emissions [United States Environmental Protection Agency, 2003a, 2003b] and sulfate aerosol concentrations [Malm *et al.*, 2002] across the United States. Despite these improvements in air quality, particulate matter concentrations persistently exceed existing standards in urban areas throughout North America [NARSTO, 2003]. Implementation strategies for further improvements in air quality will benefit from a better scientific understanding of aerosol sources, chemical speciation, and atmospheric transformations and further evaluation and development

<sup>1</sup>Also at Joint Institute for the Study of the Atmosphere and Ocean (JISAO), University of Washington, Seattle, Washington, USA.

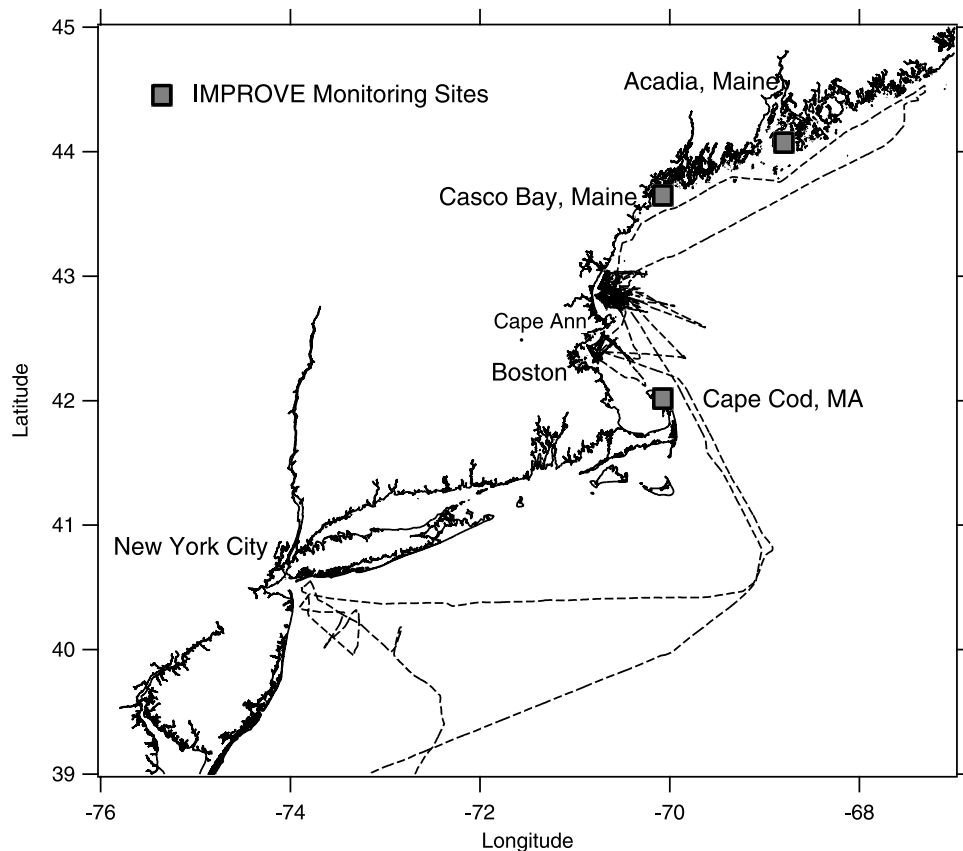


**Figure 1.** Ronald H. Brown NEAQS 2002 cruise track and locations of the coastal IMPROVE monitoring sites.

of emission and chemical transport models [NARSTO, 2003].

[3] The New England Air Quality Study (NEAQS 2002) (<http://www.al.noaa.gov/neaqs>) was conducted in July and August 2002 to assess the concentrations, transport and transformation of gases and aerosols in the marine boundary layer off the northeast coast of the United States (Figure 1). The Washington, D.C./New York City/Boston urban corridor is a source of pollutants and their precursors to coastal New England. In this paper we discuss the dominant chemical components of the aerosol particles over the Gulf of Maine from July 12 through August 10, 2002 and their role in light scattering. The NEAQS data are currently being used to evaluate and further develop emission and chemical transport models. The end goals of the project are to develop an air quality forecasting capability and to provide a better scientific understanding for air quality/climate policy decisions.

## 2. Methods

### 2.1. Aerosol Sample Inlet

[4] Aerosol particles were sampled 18m above the sea surface through a heated mast that extended 5 m above the aerosol measurement container. The mast was capped with a horizontal inlet nozzle that was rotated into the relative wind to maintain nominally isokinetic flow and minimize the loss of supermicrometer particles. Air entered the inlet through a 5 cm diameter hole, passed through a 7 degree

expansion cone, and then into the 20 cm inner diameter sampling mast. The flow through the mast was  $1 \text{ m}^3 \text{ min}^{-1}$ . The transmission efficiency for particles with aerodynamic diameters less than  $6.5 \mu\text{m}$  (the largest size tested) is greater than 95% [Bates *et al.*, 2002].

[5] The bottom 1.5 meters of the mast were heated to establish a stable reference relative humidity (RH) for the sample air of  $55 \pm 5\%$ . A stable reference RH allows for constant instrumental size segregation in spite of variations in ambient RH and results in chemical, physical, and optical measurements which are directly comparable. In addition, measurement at a constant reference RH makes it possible, with the knowledge of appropriate growth factors, for end users of the data set (process, chemical transport, and radiative transfer models) to adjust the measured parameters to a desired relative humidity. A reference RH of 55% was chosen because it is above the crystallization humidity of most aerosol components and component mixtures [Carrico *et al.*, 2003]. For the atmospheric conditions encountered during NEAQS 2002, it was possible to maintain 55% RH without excessive heating of the aerosol. On average, the aerosol was heated  $5.1^\circ\text{C}$  above the ambient temperature. For the continuous flow instruments (e.g., AMS, nephelometers) the aerosol was heated for approximately 2 sec. The temperature in the AMS sampling line was constant during the study at  $24 \pm 0.5^\circ\text{C}$ , resulting in a varying relative humidity for the AMS sampling line (average AMS RH =  $63 \pm 12\%$ ). All the other results of the in situ measurements are reported

at  $55 \pm 5\%$  RH. All references to time are reported here in UTC. Dates are given as Day of Year (DOY) where noon on February 1 equals DOY 32.5.

## 2.2. Aerosol Chemical Composition

### 2.2.1. Impactor Sample Collection for Chemical Analysis

[6] Twenty-one 1.6 cm outer diameter stainless steel tubes extended into the heated portion of the mast. These were connected to the aerosol instrumentation and impactors with conductive silicon tubing to prevent electrostatic loss of particles or stainless steel tubing for the lines to the impactors used for collection of carbonaceous aerosol and the aerosol mass spectrometer (AMS).

[7] The air flow to the impactors was controlled so that air was sampled only when the concentration of particles greater than 15 nm in diameter indicated the sample air was free of local contamination (i.e., there were no rapid increases in particle concentration), the relative wind speed was greater than  $3 \text{ m s}^{-1}$ , and the relative wind was forward of the beam.

[8] One and two-stage multijet cascade impactors [Berner *et al.*, 1979] sampling air at  $55 \pm 5\%$  RH were used to determine submicrometer and supermicrometer concentrations of inorganic ions, organic and elemental carbon (OC and EC), and inorganic oxidized material (IOM). The 50% aerodynamic cutoff diameters of the impactors,  $D_{50,\text{aero}}$ , were 1.1 and 10  $\mu\text{m}$ . The RH of the sampled air stream was measured a few inches upstream from the impactors. Throughout the paper submicrometer refers to particles with  $D_{\text{aero}} < 1.1 \mu\text{m}$  at 55% RH and supermicrometer refers to particles with  $1.1 \mu\text{m} < D_{\text{aero}} < 10 \mu\text{m}$  at 55% RH. Seven-stage multijet cascade impactors ( $D_{50,\text{aero}}$  of 0.18, 0.31, 0.55, 1.1, 2.0, 4.1, and 10  $\mu\text{m}$ ) were used to determine inorganic ion, OC and EC mass size distributions. Sampling periods ranged from 2.5 to 12 hours for all impactor samples.

[9] For inorganic ions and trace metals, the 12  $\mu\text{m}$  grease cup at the inlet of each impactor was coated with silicone grease to prevent the bounce of larger particles onto the downstream stages. A Tedlar film placed on the impactor jet plate having a  $D_{50,\text{aero}}$  of 10  $\mu\text{m}$  was sprayed with silicone lubricant for the same reason. All handling of the substrates was done in an  $\text{NH}_3$ - and  $\text{SO}_2$ -free glove box. Blank levels were determined by loading an impactor with substrates but not drawing any air through it.

### 2.2.2. Impactor Sampling for Inorganic Ions

[10] Submicrometer and supermicrometer concentrations of  $\text{Cl}^-$ ,  $\text{NO}_3^-$ ,  $\text{SO}_4^{2-}$ , methanesulfonate ( $\text{MSA}^-$ ),  $\text{Na}^+$ ,  $\text{NH}_4^+$ ,  $\text{K}^+$ ,  $\text{Mg}^{+2}$ , and  $\text{Ca}^{+2}$  were determined by ion chromatography (IC) [Quinn *et al.*, 1998]. Tedlar films were used as the collection substrate in the impaction stage and a Millipore Fluoropore filter (1.0- $\mu\text{m}$  pore size) was used for the backup filter. Prior to sampling, films were cleaned in an ultrasonic bath in 10%  $\text{H}_2\text{O}_2$  for 30 min, rinsed in distilled, deionized water, and dried in the glove box. Post sampling, filters and films were wetted with 1 mL of spectral grade methanol. An additional 5 mLs of distilled deionized water were added to the solution and the substrates were extracted by sonicating for 30 min.

[11] Non-sea-salt sulfate concentrations were calculated from  $\text{Na}^+$  concentrations and the ratio of sulfate to sodium

in seawater. Sea salt aerosol concentrations were calculated as

$$\text{sea salt}(\mu\text{g m}^{-3}) = \text{Cl}^-(\mu\text{g m}^{-3}) + \text{Na}^+(\mu\text{g m}^{-3}) \times 1.47 \quad (1)$$

where 1.47 is the seawater ratio of  $(\text{Na}^+ + \text{K}^+ + \text{Mg}^{+2} + \text{Ca}^{+2} + \text{SO}_4^{2-} + \text{HCO}_3^-)/\text{Na}^+$  [Holland, 1978]. This approach prevents the inclusion of non-sea-salt  $\text{K}^+$ ,  $\text{Mg}^{+2}$ ,  $\text{Ca}^{+2}$ ,  $\text{SO}_4^{2-}$ , and  $\text{HCO}_3^-$  in the sea salt mass and allows for the loss of  $\text{Cl}^-$  mass through  $\text{Cl}^-$  depletion processes. It also assumes that all measured  $\text{Na}^+$  and  $\text{Cl}^-$  is derived from seawater. Results of Savoie and Prospero [1980] indicate that soil dust has a minimal contribution to measured soluble sodium concentrations.

[12] Sources of uncertainty in the ionic mass include the air volume sampled ( $\pm 5\%$ ), the extract liquid volume ( $\pm 3.3\%$ ), 2 times the standard deviation of the blank values measured over the course of the experiment, and the precision of the method (2 times the standard deviation of repeated injections of a single sample). The overall uncertainty in the ionic mass at the 95% confidence level, propagated as a quadratic sum of all the errors, was  $\pm 11\%$  for a concentration of  $10 \mu\text{g m}^{-3}$ .

### 2.2.3. Impactor Sampling for Organic and Elemental Carbon

[13] Submicrometer and sub-10  $\mu\text{m}$  samples were collected using 2 and 1 stage impactors, respectively. Each impactor had two quartz backup filters. The sub-10  $\mu\text{m}$  and one submicrometer impactor were run without a denuder upstream. A second submicrometer impactor was run with a denuder upstream. The denuder was 30 cm long, contained 18 parallel strips of carbon-impregnated glass (CIG) fiber filters separated by 1.8 mm, and had a cross-sectional area of  $9.6 \text{ cm}^2$ . A seven-stage multijet cascade impactor was used to determine OC and EC mass size distributions. Aluminum foils were used for the impaction substrates and 47 mm quartz filters were used as the backup filters. All substrates were prebaked at  $500^\circ\text{C}$  prior to sampling.

[14] The OC/EC sampling strategy incorporated various combinations of denuders, impactors, and filters. The submicrometer OC data are from the denuder/impactor sampler. The last backup quartz filter in line was used as the blank. The supermicrometer OC data are the difference between the sub-10  $\mu\text{m}$  and submicrometer impactors run without denuders. Impactors without denuders upstream were used for the supermicrometer OC determination in order to avoid losses of large particles in the denuder. OC concentrations from all impactors were corrected for blanks and artifacts using the last quartz filter in line. Submicrometer EC data are the average of the two submicrometer impactor samples (with and without denuders). Supermicrometer EC data are the difference between the sub-10  $\mu\text{m}$  and the average of the two submicrometer impactor samples (with and without denuders).

[15] OC and EC concentrations were determined with a Sunset Laboratory thermal/optical analyzer. The thermal program was the same as that used in ACE Asia [Mader *et al.*, 2003; Schauer *et al.*, 2002]. Four temperature steps were used to achieve a final temperature of  $870^\circ\text{C}$  in He to drive off OC. After cooling the sample down to  $550^\circ\text{C}$ , a He/ $\text{O}_2$  mixture was introduced and the sample was heated in four temperature steps to  $910^\circ\text{C}$  to drive off EC. The

transmission of light through the filter was measured to separate EC from any OC that charred during the initial stages of heating. No correction was made for carbonate carbon so OC includes both organic and carbonate carbon. Since an optically detected split point between OC and EC can not be used with the AI impactor foils, the split between OC and EC in the 7-stage impactors was based on a split time for the stage 1 quartz filter.

[16] The mass of particulate organic matter (POM) was determined by multiplying the measured organic carbon concentration in  $\mu\text{g m}^{-3}$  by a factor of 1.6. The POM factor is an estimated average of the molecular weight per carbon weight and is based on a review of published measurements of the composition of organic aerosol in urban and nonurban regions [Turpin and Lim, 2001]. Based on the range of values given by Turpin and Lim [2001], the POM factor has an uncertainty of  $\pm 31\%$ .

[17] The uncertainties associated with positive and negative artifacts in the sampling of semi-volatile organic species can be substantial. Based on the results of Mader et al. [2003], the submicrometer OC was measured with a denuder upstream to minimize positive (adsorption of gas phase species) artifacts. Other sources of uncertainty in the POM mass include the air volume sampled ( $\pm 5\%$ ), the area of the filter ( $\pm 5\%$ ), 2 times the standard deviation of the blanks measured over the course of the experiment ( $0.44 \mu\text{g cm}^{-2}$ ), the precision of the method ( $\pm 5\%$ ) based on the results of Schauer et al. [2002], and the POM factor (31%). A quadratic sum of all errors involved yields a 95% uncertainty of  $\pm 37\%$  for an OC mass of  $8.6 \mu\text{g C cm}^{-2}$ .

[18] Sources of uncertainty in the EC mass include the air volume sampled ( $\pm 5\%$ ), the area of the filter ( $\pm 5\%$ ), and the precision of the method ( $\pm 13\%$ ) based on the results of Schauer et al. [2002]. A quadratic sum of all errors involved yields a 95% uncertainty of  $\pm 24\%$  for an EC mass of  $1 \mu\text{g C cm}^{-2}$ .

#### 2.2.4. Impactor Sampling for Inorganic Oxidized Material (Dust) and Gravimetrically Determined Mass

[19] Total elemental composition (Na, Mg, Al, Si, P, Cl, K, Ca, Ti, V, Cr, Mn, Fe, Ni, Cu, Zn, Ba, As, and Pb) was determined by thin-film x-ray primary and secondary emission spectrometry. Submicrometer and sub- $10 \mu\text{m}$  samples were collected on  $1.0 \mu\text{m}$  pore size Teflo filters using 2 and 1 stage impactors, respectively. Supermicrometer elemental concentrations were determined by the difference between the submicrometer and sub- $10 \mu\text{m}$  samples. Filters were weighed before and after sample collection as described below.

[20] A component composed of inorganic oxidized material (IOM) was constructed from the elemental data. The IOM most likely was composed of soil dust and/or fly ash. These two components are difficult to distinguish based on elemental ratios. To construct the IOM component, the mass concentrations of Al, Si, Ca, Fe, and Ti, the major elements in soil and fly ash, were combined. It was assumed that each element was present in the aerosol in its most common oxide form ( $\text{Al}_2\text{O}_3$ ,  $\text{SiO}_2$ ,  $\text{CaO}$ ,  $\text{K}_2\text{O}$ ,  $\text{FeO}$ ,  $\text{Fe}_2\text{O}_3$ ,  $\text{TiO}_2$ ). The measured elemental mass concentration was multiplied by the appropriate molar correction factor as follows:

$$[\text{IOM}] = 2.2[\text{Al}] + 2.49[\text{Si}] + 1.63[\text{Ca}] + 2.42[\text{Fe}] + 1.94[\text{Ti}] \quad (2)$$

[Malm et al., 1994; Perry et al., 1997]. This equation includes a 16% correction factor to account for the presence of oxides of other elements such as K, Na, Mn, Mg, and V that are not included in the linear combination. In addition, the equation omits K from biomass burning by using Fe as a surrogate for soil K and an average K/Fe ratio of 0.6 in soil [Cahill et al., 1986].

[21] Sources of uncertainty in the IOM mass concentration include the volume of air sampled ( $\pm 5\%$ ), the area of the filter ( $\pm 5\%$ ), the molar correction factor ( $\pm 6\%$ ), 2 times the standard deviation of the blank values measured over the course of the experiment for each element, and the precision of the X-ray analysis [Feely et al., 1991]. The overall uncertainty in the IOM mass, propagated as a quadratic sum of all the errors involved, was  $\pm 6\%$  for a concentration of  $70 \mu\text{g m}^{-3}$ .

[22] Films and filters were weighed at PMEL with a Cahn Model 29 and Mettler UMT2 microbalance, respectively. The balances are housed in a glove box kept at a humidity of  $55 \pm 2\%$ . The resulting mass concentrations from the gravimetric analysis include the water mass that is associated with the aerosol at 55% RH. The glove box was continually purged with room air that had passed through a scrubber of activated charcoal, potassium carbonate, and citric acid to remove gas phase organics, acids, and ammonia. Static charging, which can result in balance instabilities, was minimized by coating the walls of the glove box with a static dissipative polymer (Tech Spray, Inc.), placing an antistatic mat on the glove box floor, using antistatic gloves while handling the substrates, and exposing the substrates to a  $^{210}\text{Po}$  source to dissipate any charge that had built up on the substrates. Before and after sample collection, substrates were stored double-bagged with the outer bag containing citric acid to prevent absorption of gas phase ammonia. More details of the weighing procedure can be found in Quinn and Coffman [1998]. The uncertainty at the 95% confidence level was  $\pm 11\%$  for a mass concentration of  $20 \mu\text{g m}^{-3}$ . Concentrations are reported as  $\mu\text{g m}^{-3}$  at STP ( $25^\circ\text{C}$  and 1 atm).

#### 2.2.5. Aerosol Chemical Measurements From the Aerodyne Mass Spectrometer

[23] Chemically classified and size-resolved mass loadings of submicrometer aerosol were measured using an Aerosol Mass Spectrometer (AMS) developed at Aerodyne Research, Inc. (Billerica, Massachusetts, USA) [Jayne et al., 2000; Allan et al., 2003]. The AMS measured both the mass concentrations of chemical species and the vacuum aerodynamic size ( $D_{va}$ ) of the particles. The vaporized species analyzed by the AMS are referred to as non-refractory (NR), and are defined as all chemical components that vaporize ( $< 5 \text{ s}$ ) at the vaporizer temperature of  $\sim 550^\circ\text{C}$ . This includes most organic carbon species and inorganic species such  $\text{NH}_4\text{NO}_3$  and  $(\text{NH}_4)_x\text{H}_y\text{SO}_4$  but does not include crustal oxides, elemental carbon, or sea salt. Details of the AMS operation, calibration, and measurements made on board Ronald H. Brown during NEAQS 2002 can be found in A. M. Middlebrook et al. (manuscript in preparation, 2004). Briefly, the AMS collection efficiencies were determined for each leg of the cruise based on the average slopes of linear regressions with the particle into liquid sampler (PILS) ion chroma-

tography measurements of sulfate and ammonium (with  $r^2 = 0.9$  for all four regressions): the collection efficiencies were 0.61 for leg one and 0.93 for leg two of the cruise. Although many factors contribute to the AMS collection efficiency, the low collection efficiency for leg one was due to a significant difference in the mass between the cut points of the AMS and PILS as well as a lower average relative humidity in the AMS sampling line. The collection efficiency for each leg was used for sulfate, POM, nitrate and ammonium, assuming an internally mixed aerosol. A singular value decomposition linear regression of the AMS POM measurements with the impactor OC measurements (section 2.2.3) for the data used in this analysis yielded a line with an  $r^2 = 0.85$  and a slope of  $1.74 \pm 0.14$ . This implies a POM/OC factor of 1.7 rather than the 1.6 used in the data analysis discussed in this paper. However, an independent analysis of the AMS data, accounting for the carbon mass fraction at each mass to charge ratio in the spectra, resulted in a study average POM/OC factor of 1.62 which is consistent with the factor of 1.6 used in this paper and from previous studies [Quinn and Bates, 2005]. While this factor may vary depending on the age of the aerosol, we found that for most of this study the POM was oxidized and was predominantly formed via secondary processing [de Gouw et al., 2005]. The uncertainty in the AMS concentration measurements during NEAQS 2002 was estimated at  $\pm 20\%$ .

### 2.3. Ozone and Sulfur Dioxide

[24] Air was pulled from 18 m above sea level down the 20 cm ID powder-coated aluminum aerosol sampling mast (6 m) at approximately  $1 \text{ m}^3 \text{ min}^{-1}$ . At the base of the sampling mast a  $0.5 \text{ L min}^{-1}$  flow was pulled through a 0.32 cm ID, 2m long Teflon tube into a TECO 49 ozone analyzer that had been calibrated to a NIST traceable analyzer at NOAA-CMDL. Data were recorded as one minute averages.

[25] Similarly, at the base of the sampling mast a  $0.5 \text{ L min}^{-1}$  flow was pulled through a 0.32 cm inner diameter, 1m long Teflon tube, a Millipore Fluoropore filter (1.0- $\mu\text{m}$  pore size) housed in a Teflon filter holder, a Perma Pure Inc. Nafion Drier (MD-070, stainless steel, 61 cm long) and then through 2 m of Teflon tubing to a Thermo Environmental Instruments Model 43C Trace Level Pulsed Fluorescence  $\text{SO}_2$  Analyzer. The initial 1 m of tubing, filter and drier were located in the humidity controlled (55%) chamber at the base of the mast. Dry zero air (scrubbed with a charcoal trap) was run through the outside of the Nafion Drier at  $1 \text{ L min}^{-1}$ . The analyzer was run with two channels (0–20 ppb full scale and 0–100 ppb full scale) and a 20 sec averaging time. Data were recorded every minute.

[26] Zero air was introduced into the sample line upstream of the Fluoropore filter for 10 minutes every hour to establish a zero baseline. An  $\text{SO}_2$  standard was generated with a permeation tube held at  $50^\circ\text{C}$ . The flow over the permeation tube, diluted to 4.0 ppb, was introduced into the sample line upstream of the Fluoropore filter for 10 minutes every 6 hours. The limit of detection for the 1 min data, defined as 2 times the standard deviation of the signal during the zero periods, was 100 ppt. Uncertainties in the

concentrations based on the permeation tube weight and dilution flows is  $<5\%$ .

### 2.4. Aerosol Light Scattering

[27] Measurements of aerosol scattering and hemispheric backscattering coefficients were made with an integrating nephelometer (Model 3563, TSI Inc.) at wavelengths of 450, 550, and 700 nm. The sample RH was measured in the center of the nephelometer sensing volume using a custom installed capacitive type RH sensor (Vaisala model HMP135Y). Two single stage impactors, one with  $D_{50,\text{aero}}$  of  $1.1 \mu\text{m}$  and one with a  $D_{50,\text{aero}}$  of  $10 \mu\text{m}$ , were placed upstream of the nephelometer. An automated valve switched between the two impactors every 15 min so that sampling alternated between submicrometer and sub- $10 \mu\text{m}$  aerosol. Values measured by the nephelometer were corrected for an offset determined by measuring filtered air over a period of several hours.  $\text{CO}_2$  was used as the span gas. Measurements of filtered air and  $\text{CO}_2$  were made every 2 to 3 days. In addition, submicrometer and supermicrometer values were corrected separately for angular non-idealities of the nephelometer, including truncation errors and non-lambertian illumination, using the method of Anderson and Ogren [1998]. Values are reported at  $0^\circ\text{C}$  and 1013 mb. For a 30 min averaging time and a wavelength of 550 nm, a quadrature sum of errors yielded relative uncertainties at the 95% confidence level of  $\pm 14\%$ .

### 2.5. Number Size Distributions

[28] One of the 21 mast tubes was used to supply ambient air to an ultrafine differential mobility particle sizer (UDMPS), a differential mobility particle sizer (DMPS) and an aerodynamic particle sizer (APS, TSI model 3320). The two DMPSs were located in a humidity-controlled box (RH =  $55 \pm 5\%$ ) at the base of the mast. The UDMPS was a short column instrument connected to a TSI 3025 particle counter (TSI, St. Paul, MN) operating with a positive center rod voltage to sample particles with a negative charge. Data were collected in 17 size bins from 3 to 26 nm geometric diameter. The UDMPS operated with an aerosol flow rate of  $1 \text{ L min}^{-1}$  and a sheath air flow rate of  $10 \text{ L min}^{-1}$ . The DMPS was a medium length column instrument connected to a TSI 3760 particle counter operating with a positive center rod voltage to sample particles with a negative charge. Data were collected in 17 size bins from 20 to 671 nm diameter. The DMPS operated with an aerosol flow rate of  $0.5 \text{ L min}^{-1}$  and a sheath air flow rate of  $5 \text{ L min}^{-1}$ . The relative humidity of the sheath air for both DMPSs was controlled resulting in a measurement RH in the DMPSs of approximately 55%. With this RH control the aerosol should not have effloresced if it was hydrated in the atmosphere [Carrico et al., 2003]. Mobility distributions were collected every 15 minutes.

[29] The mobility distributions from the UDMPS and DMPS were inverted to a number distribution assuming a Fuchs-Boltzman charge distribution from the  $\text{Kr}^{85}$  charge neutralizer. The overlapping channels between the two instruments were eliminated in the inversion. The data were corrected for diffusional losses and size dependent counting efficiencies based on pre-ACE-2 intercalibration exercises. The estimated uncertainty in the number concentration in each bin, based on flow uncertainties is  $\pm 10\%$ .

**Table 1.** Measured and Calculated Submicrometer Aerosol Light Scattering Coefficients (550 nm) at 55% RH for Northwesterly and Southwesterly Flows<sup>a</sup>

	Northwesterly	Southwesterly
Measured (nephelometer)	27 ± 16	104 ± 40
Calculated (DMPS and impactors)		
POM	15 ± 6.8	40 ± 15
(NH <sub>4</sub> ) <sub>x</sub> H <sub>y</sub> SO <sub>4</sub> -H <sub>2</sub> O	7.2 ± 6.1	52 ± 23
Other	3.6 ± 1.9	11 ± 5.3
Total all components	26 ± 13	102 ± 36
Calculated (AMS)		
POM	18 ± 6.7	46 ± 16
(NH <sub>4</sub> ) <sub>x</sub> H <sub>y</sub> SO <sub>4</sub> -H <sub>2</sub> O	4.9 ± 3.2	50 ± 28
Total POM + (NH <sub>4</sub> ) <sub>x</sub> H <sub>y</sub> SO <sub>4</sub> -H <sub>2</sub> O	23 ± 7.5	96 ± 32

<sup>a</sup>Units are in Mm<sup>-1</sup>. Values given are regional means ± 1 σ standard deviation.

[30] The APS was located in the lower humidity controlled box (55 ± 5% RH) at the base of the mast. Modifications were made to the APS to account for the internal heating of the sample in the APS by its sheath flow and waste heat, which could reduce the measurement RH below 55% RH. First, the sheath flow was conditioned outside the instrument case before reintroduction into the sheath and acceleration nozzle. Second, the inlet tube was insulated to reduce heating at that point. While the temperature at the APS's sensing volume was not measured during sampling, laboratory testing prior to the cruise showed a significant reduction in the internal heating. Before the modifications, the differential temperature in between the inlet and the sensing volume was about 3°C, but after the modifications, the same differential temperature was reduced to less than 1°C.

[31] Number size distributions were collected with the APS every 15 minutes averaged over the 13 minutes of the DMPS scan. The APS data were collected in 51 size bins with the nominal manufacturers aerodynamic diameters ranging from 0.542 to 20 μm. Data were corrected for phantom counts assuming that the counts in the largest 4 channels ( $D_{\text{aero}} = 16$  to 20 μm) were phantom counts and that value was subtracted from the entire APS distribution. This correction resulted in a Junge slope of the number distribution that was nearly constant for  $D_p > 5$  μm and a volume concentration that varied randomly about zero for  $D_p > 10$  μm. The APS data were corrected for ultra-Stokesian conditions in the instrument jet [Wang and John, 1987; Cheng et al., 1993]. Finally, the APS data were converted from aerodynamic diameters to geometric diameters using calculated densities and the water masses associated with the inorganic ions at 55% RH. The densities and associated water masses were calculated with a thermodynamic equilibrium model (AeRho) using the measured chemical data [Quinn et al., 2002]. The estimated uncertainty in the supermicrometer size distribution include particle sizing (±3%) and the instrumental counting efficiency (±5%).

## 2.6. Back Trajectories

[32] Air mass back trajectories were calculated at four arrival altitudes (100, 500, 2500, and 5500 m) for the ship's position at six hour intervals using the hybrid-coordinate model HY-SPLIT 4 using the EDAS meteorological data set [Draxler, 1992]. The trajectories were

used to divide the measurements into the two source region groups.

## 2.7. Calculations of Aerosol Water Content and Mass Scattering Efficiency

[33] The chemical thermodynamic equilibrium model AeRho was used to estimate the water mass associated with the inorganic ions at 55% RH. It was assumed that the inorganic aerosol was an internal mixture containing all measured ionic species. The chemical reactions allowed to occur, the crystallization humidities used for the solid phase species, and the method for the calculation of the aerosol water content are given in Quinn et al. [2002]. Both the IOM and the organic mass were assumed to not take up any water. AeRho was also used to calculate the refractive index and density for each chemical component based on measured size distributions and chemical composition. To check for internal consistency in the measured and modeled parameters, closure experiments were performed for measured and calculated mass and scattering (summarized in section 3.1 and Table 1).

[34] The fraction of the measured light scattering due to the dominant chemical components was calculated at 55% RH and 550 nm using a Mie model and measured number size distributions and size segregated (impactor) chemical mass concentrations. The components included sea salt (which includes supermicrometer NO<sub>3</sub><sup>-</sup> and associated H<sub>2</sub>O), nss sulfate aerosol (which included nss SO<sub>4</sub><sup>-</sup>, NH<sub>4</sub><sup>+</sup>, and associated H<sub>2</sub>O), IOM or dust, POM (derived from OC assuming an OC to POM factor of 1.6), and EC (which included submicrometer nss K<sup>+</sup> with associated nss SO<sub>4</sub><sup>-</sup>). The IOM, POM, and EC components were assumed to be hydrophobic. The calculations were also done using the AMS mass distributions using two components, nss sulfate aerosol (which included the measured nss SO<sub>4</sub><sup>-</sup> and NH<sub>4</sub><sup>+</sup>, and calculated associated H<sub>2</sub>O) and POM (measured directly by the AMS). Mass scattering efficiencies of the individual chemical components (m<sup>2</sup> g<sup>-1</sup>), defined as

$$\text{MSE}_j = \sigma_{\text{sp},j}/m_j \quad (3)$$

where  $\sigma_{\text{sp},j}$  is the light scattering due to component  $j$  and  $m_j$  is the mass concentration of the component or ion, were estimated from the calculated component scattering and measured mass concentrations of the chemical components. Details of the Mie calculations can be found in Quinn et al. [2002]. Aerosol light absorption and single scattering albedos are reported in Quinn and Bates [2003] and Quinn and Bates [2005].

## 3. Results and Discussion

### 3.1. Regional Aerosol Chemical Composition

[35] The submicrometer aerosol mass of chemically analyzed components ranged from 2 to 35 μg m<sup>-3</sup> (Figure 2a) and was dominated by NH<sub>4</sub><sup>+</sup>, non-sea-salt (nss) SO<sub>4</sub><sup>-</sup>, and POM. The urban plumes from New York City and Boston were clearly seen above the background concentration on DOY 197, 200, 203–205, 211, and 216–218. The ammonium sulfate aerosol was acidic in 42 out of 46 samples with a mean NH<sub>4</sub><sup>+</sup>/nssSO<sub>4</sub><sup>-</sup> molar ratio of 1.7 ± 0.3 (range: 0.26 to 2.1). The chemically analyzed submicrometer mass

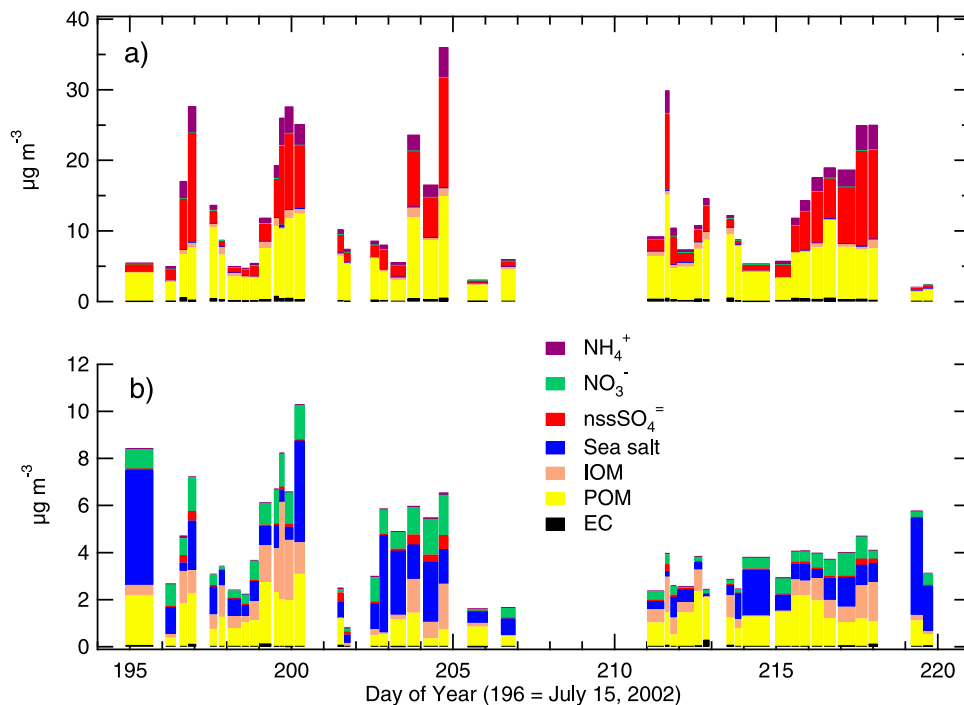


**Figure 2.** The (a) submicron and (b) supermicron aerosol mass of chemically analyzed components.

plus associated water accounted for  $94 \pm 11\%$  of the gravimetric mass.

[36] The supermicrometer aerosol mass of chemically analyzed components ranged from 0.3 to  $10 \mu\text{g m}^{-3}$  (Figure 2b) and was compositionally quite different from the submicrometer mass. The dominant chemical components included  $\text{NO}_3^-$ , sea salt, dust, and POM. The chemically analyzed supermicrometer mass accounted for  $90 \pm 18\%$  of the gravimetric mass. The supermicrometer mass during NEAQS 2002 was only  $25 \pm 7.9\%$  of the sub  $10 \mu\text{m}$  aerosol dry mass and was lower than that measured in marine conditions [Quinn and Bates, 2005] due to the low wind speeds ( $5.1 \pm 2.3 \text{ m s}^{-1}$ ) and short fetch encountered during the experiment.

[37] The air masses sampled in the Gulf of Maine during NEAQS 2002 can be divided into two groups based on the synoptic meteorology [Miller and Keim, 2003]. When the region was under the influence of a high pressure system over Canada (approximately 50% of the time), the surface winds were from the north to northwest bringing air from northern New England and Canada. When the region was under the influence of a weak low pressure center over northern Ontario and/or Quebec (approximately 30% of the time), the surface winds ahead of the front were from the southwest (J. P. Koerner et al., manuscript in preparation, 2004). Under these conditions the air mass sampled at the ship had passed over the urban New York/Boston corridor during the previous 2–24 hours. The latter conditions led to high pollution episodes (afternoon ozone concentrations in excess of 100 ppb) along the New England coast.

[38] Under both synoptic conditions the submicrometer aerosol consisted primarily ( $92 \pm 4\%$  of the total dry mass) of  $(\text{NH}_4)_x\text{H}_y\text{SO}_4$  and POM. Under northwesterly flow (Figure 3b), POM was the dominant component ( $68 \pm 8\%$ ) followed by  $(\text{NH}_4)_x\text{H}_y\text{SO}_4$  ( $23 \pm 8\%$ ), IOM ( $6 \pm 4\%$ ), and

EC ( $3 \pm 1\%$ ). Under southwesterly flow (Figure 3a),  $(\text{NH}_4)_x\text{H}_y\text{SO}_4$  was the dominant component ( $54 \pm 9\%$ ) followed by POM ( $41 \pm 9\%$ ), IOM ( $3 \pm 2\%$ ) and EC ( $2 \pm 1\%$ ). While the large fraction of  $(\text{NH}_4)_x\text{H}_y\text{SO}_4$  is not surprising [Malm et al., 2004], the large fraction of POM is not typical of most continental plumes advecting out over the oceans [Quinn and Bates, 2005]. Based on the IMPROVE data set collected from March 2001 to February 2002, Malm et al. [2004] concluded that the mass fraction of sulfate in the eastern United States was 60 to nearly 80%. However, the IMPROVE coastal chemical data from the three stations around the Gulf of Maine (Acadia, Maine; Casco Bay, Maine; Cape Cod, Massachusetts) averaged over July and August 2002 (<http://vista.cira.colostate.edu/improve/>) are consistent with the data collected on the ship during NEAQS 2002 southwesterly flow (Figure 4). The 24 hour samples collected every three days at the three coastal IMPROVE sites had average POM concentrations  $>40\%$ . In addition,  $>50\%$  of the samples had  $>40\%$  POM (POM factor of 1.6). Note, however, that the IMPROVE data are sub- $2.5 \mu\text{m}$  at ambient humidity and thus include some of the supermicrometer aerosol.

[39] During NEAQS 2002 the supermicrometer mass under both northwesterly (Figure 5b) and southwesterly (Figure 5a) flows had a large POM component ( $41 \pm 14\%$  and  $26 \pm 13\%$ , respectively), a sea-salt/ $\text{NaNO}_3$  component ( $36 \pm 19\%$  and  $41 \pm 15\%$ ), and an IOM component ( $18 \pm 12\%$  and  $26 \pm 11\%$ ). The slightly higher  $(\text{NH}_4)_x\text{H}_y\text{SO}_4$  and  $\text{NO}_3^-$  components in the southwesterly flows are consistent with the enhanced urban sources along these trajectories.

[40] Previous studies have also measured high concentrations of organic aerosol advecting off the east coast of North America. Novakov et al. [1997] and Putaud et al. [2000] measured average free troposphere POM/ $(\text{NH}_4)_x\text{H}_y\text{SO}_4$

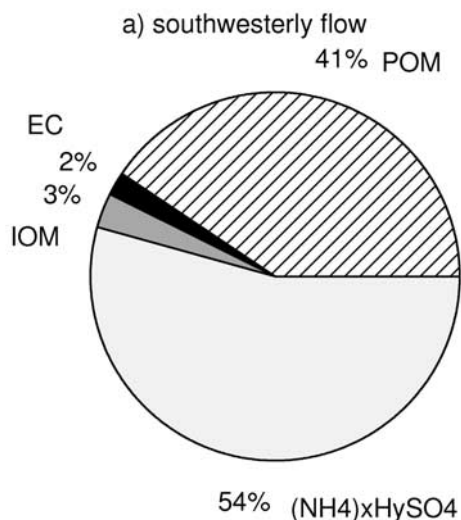


**Figure 3a.** Mass fractions of dominant submicron chemical components during southwesterly flow. The average gravimetric mass at 55% RH was  $30 \pm 11 \mu\text{g m}^{-3}$ .

ratios of 3.7 (POM factor of 1.6) compared to 2.9 and 0.73 measured in the NEAQS NW and SW flows, respectively. Novakov *et al.* [1997] showed that the carbon mass fraction during TARFOX tended to increase with altitude. The mean POM/(NH<sub>4</sub>)<sub>x</sub>HySO<sub>4</sub> ratio in the lower atmosphere ( $\leq 1.0$  km) during TARFOX was  $0.90 \pm 0.45$  [Hegg *et al.*, 1997].

## 3.2. Regional Aerosol Sources

### 3.2.1. Aerosol nssSO<sub>4</sub><sup>-</sup> and NO<sub>3</sub><sup>-</sup>

[41] The sources of nssSO<sub>4</sub><sup>-</sup> aerosol in the Northeast have been well documented and are consistent with regional SO<sub>2</sub> sources, primarily power plant emissions [Malm *et al.*, 2002, and references therein]. Both SO<sub>2</sub> and SO<sub>4</sub><sup>-</sup> concentrations decreased by 28% in the Northeast (Illinois to Maine) during the 1990s as a result of the reduction in emissions from utilities participating in the Phase I implementation of the Acid Rain Program [Malm *et al.*, 2002]. The NO<sub>3</sub><sup>-</sup> aerosol ( $0.67 \pm 0.46 \mu\text{g m}^{-3}$ ) measured during NEAQS 2002 was primarily in the supermicrometer fraction along with sea salt. The supermicrometer sea salt aerosol was highly depleted in chlorine with a mean Cl<sup>-</sup>/Na<sup>+</sup> molar ratio of  $0.58 \pm 0.26$  (range: 0.1 to 1.1). Unreacted sea salt has a Cl<sup>-</sup>/Na<sup>+</sup> molar ratio of 1.18. The mean supermicrometer (NO<sub>3</sub><sup>-</sup> + Cl<sup>-</sup>)/Na<sup>+</sup> molar ratio was  $1.18 \pm 0.17$  suggesting that the chloride was displaced by HNO<sub>3</sub> and/or nitrogen oxides. NO<sub>x</sub> emissions in the Northeast United States are derived largely from transportation (54%), electric utilities (25%) and industrial sources (11%) [Driscoll *et al.*, 2003]. NO<sub>x</sub> is quickly converted to HNO<sub>3</sub> as a result of both daytime and nighttime chemistry [Brown *et al.*, 2004]. Over the ocean HNO<sub>3</sub> is rapidly deposited onto sea salt aerosols and the sea surface [Brown *et al.*, 2004].

### 3.2.2. Aerosol OC and EC

[42] Non-sea-salt K<sup>+</sup>/EC mass ratios have been used as markers of biomass burning [Andreae, 1983] since nss K<sup>+</sup> is a combustion product of biomass and not fossil fuel. Although a large biomass burning event affected New England during early July 2002 prior to the study, the low

nss K<sup>+</sup>/EC ratios ( $0.11 \pm 0.05$ ) measured during NEAQS indicate that fossil fuel combustion was the main source of EC and that contributions from biomass/biofuel burning sources were insignificant [Quinn and Bates, 2005]. Concentrations of the gas phase biomass burning tracer, acetonitrile, also were low [de Gouw *et al.*, 2005] providing further evidence that biomass burning did not contribute to measured EC concentrations. Low EC/OC ratios ( $0.08 \pm 0.02$ ) and high OC/nssSO<sub>4</sub><sup>-</sup> ratios ( $1.4 \pm 1.3$ ) also suggest that the high OC aerosol concentrations measured during NEAQS 2002 were not a result of direct emissions from combustion processes but instead were produced from the atmospheric oxidation of VOCs. Monoterpene emission rates are high in the coniferous forests of northeastern North America [Guenther *et al.*, 1995], especially in the summer months [Guenther *et al.*, 2000], providing gas phase precursors for the organic aerosol. During one sampling period of NEAQS2002 high concentrations of biogenic VOCs were measured, yet the NR POM during this period was better correlated with secondary anthropogenic gas phase species [de Gouw *et al.*, 2005]. These results suggest that most of the NR POM observed during NEAQS2002 was due to secondary anthropogenic processes rather than those involving biogenic species.

## 3.3. Regional Aerosol Light Scattering

[43] The submicrometer aerosol light scattering coefficient ( $\sigma_{\text{sp}}$ ) at 550nm (RH  $55 \pm 5\%$ ) ranged from less than  $10 \text{ Mm}^{-1}$  in the cleanest air masses off the coast of Maine to  $260 \text{ Mm}^{-1}$  in the plumes downwind of the urban corridor (Figure 6), clearly following the pattern of aerosol mass. The submicrometer aerosol accounted for  $86 \pm 12\%$  of the sub-10  $\mu\text{m}$  aerosol light scattering during NEAQS 2002. A singular value decomposition least squares linear regression of  $\sigma_{\text{sp}}$  with submicrometer gravimetric mass yielded:

$$\sigma_{\text{sp}} = (3.7 \pm 0.11)[\text{submicrometer gravimetric mass}], r^2 = 0.91 \quad (4)$$

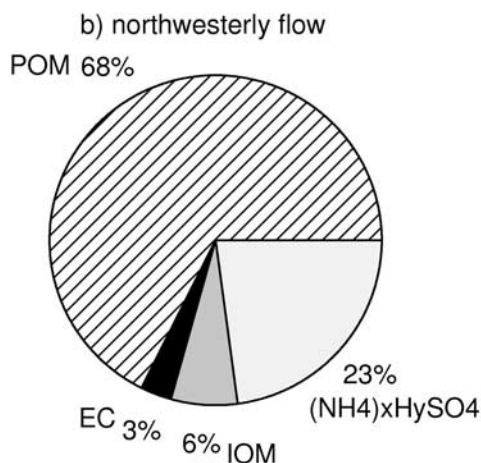


**Figure 3b.** Mass fractions of dominant submicron chemical components during northwesterly flow. The average gravimetric mass at 55% RH was  $11 \pm 4.5 \mu\text{g m}^{-3}$ .

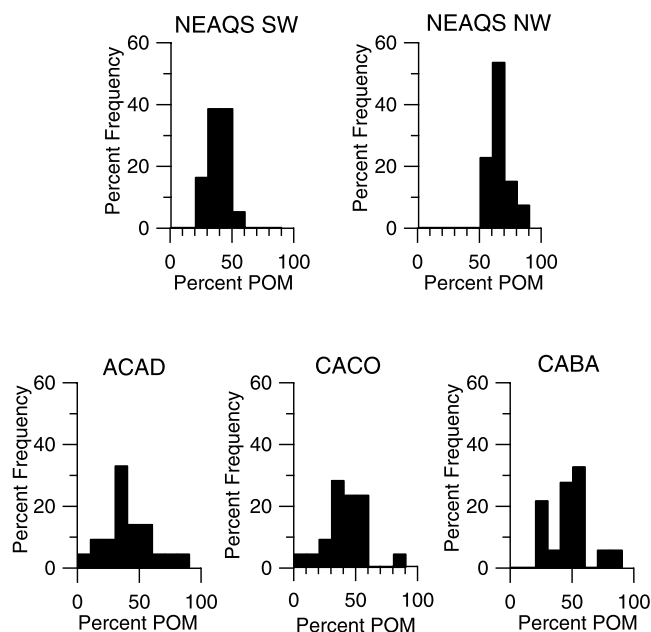


**Figure 4.** Percent frequency of percent POM in individual samples collected during NEAQS and during July and August at the three coastal IMPROVE sites (see Figure 1 for station locations: CABA, Casco Bay, Maine; ACAD, Acadia, Maine; CACO, Cape Cod, Massachusetts).

The resulting mass scattering efficiency MSE ( $3.7 \pm 0.11 \text{ m}^2 \text{ g}^{-1}$ ) is consistent with theoretical calculations using Mie theory [Boucher and Anderson, 1995; Charlson *et al.*, 1999] for a general low RH accumulation-mode aerosol.

[44] A critical question in addressing regional air quality issues is “How do the various aerosol chemical species contribute to the total aerosol light scattering?” For a multicomponent system, particle light scattering  $\sigma_{\text{sp}}$  can be modeled as a linear, humidity-independent function of the concentration of the major components of the aerosol (here  $\text{SO}_4^{2-}$  and POM) and a constant term such that

$$\sigma_{\text{sp}} = \alpha_{\text{SO}_4^{2-}} m_{\text{SO}_4^{2-}} + \alpha_{\text{POM}} m_{\text{POM}} + \alpha_1 \text{ Mm}^1 \quad (5)$$

where  $\alpha$  is the mass scattering efficiency (MSE) of the component and  $m$  is the measured mass of that component [White, 1986]. Here the  $\text{SO}_4^{2-}$  component of the aerosol is defined as  $[(\text{NH}_4)_x\text{H}_y\text{SO}_4 + \text{H}_2\text{O}]$  where  $\text{H}_2\text{O}$  is the water associated with  $(\text{NH}_4)_x\text{H}_y\text{SO}_4$  at the measured scattering RH (55%).

[45] White [1986] reviewed the complexity of apportioning extinction to internally mixed aerosol species. In this case, equation (5) can only be an approximation since the extinction efficiency of one species depends on the relative abundance of the other species. That is, the removal of one species affects the particle size of the other species. Furthermore, the removal of one species may permit additional condensation on the other species or changes in the equilibrium vapor pressure [White, 1986]. Calculations in this paper do not allow the size distribution to change with the addition or removal of one species and neglect any interaction between components.

[46] Scattering and mass scattering efficiencies of individual chemical components can be calculated from Mie theory based on measurements of mass size distributions [Ouimette and Flagan, 1982; White, 1986; Charlson *et al.*, 1999]. Mass size distributions of the chemical components were obtained during NEAQS with both 7 stage impactors and the AMS. For the more limited size resolution impactor data, the percent composition in each stage and the calculated density and associated water content (section 2.7) were applied to the number size distribution (section 2.5) to obtain number size distributions for each chemical component. The AMS mass size distributions were converted to component number size distributions after calculating a density and associated water content from the chemical composition. The scattering from each component (POM and  $(\text{NH}_4)_x\text{H}_y\text{SO}_4 + \text{H}_2\text{O}$  for the AMS and POM,  $(\text{NH}_4)_x\text{H}_y\text{SO}_4 + \text{H}_2\text{O}$ , and remaining analyzed mass for the impactor data) was then calculated. The MSEs were then obtained from the calculated component scattering (POM and  $[(\text{NH}_4)_x\text{H}_y\text{SO}_4 + \text{H}_2\text{O}]$ ) and the measured component mass from the impactors or AMS (equation (3)). Submicrometer aerosol light scattering and MSE for northwesterly and southwesterly flows are given in Tables 1 and 2, respectively. Measured and calculated scattering coefficients agreed to within the measurement and modeling uncertainties. The relative uncertainty in the calculated scattering coefficients was  $\pm 35\%$  [Quinn *et al.*, 2002, Table 3]. Scattering closure between the measured (nephelometer) and calculated (sum of the components using the DMPS/impactor size distributions) scattering coefficients was achieved well within this uncertainty ( $18 \pm 14\%$  and  $8.0 \pm 8.6\%$  for northwesterly and southwesterly flow, respectively) showing that the data set was internally consistent.

[47] The results from these calculations show that POM was the dominant scattering component during northwesterly flow ( $61 \pm 8.2$ ) and a major contributor to scattering under southwesterly flow ( $40 \pm 8.8$ ). Based on measurements north of the NEAQS study area at Sable Island,

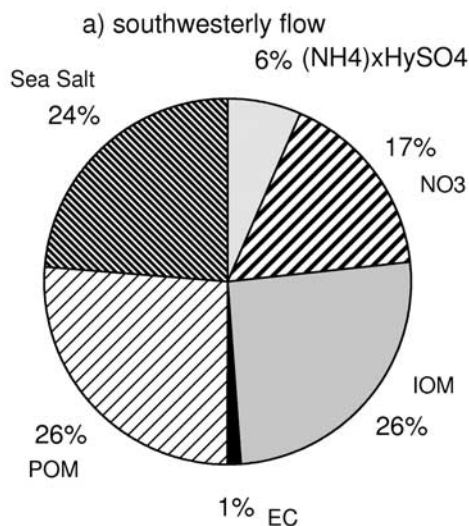


**Figure 5a.** Mass fractions of dominant supermicron chemical components during southwesterly flow. The average gravimetric mass at 55% RH was  $9.1 \pm 4.6 \text{ } \mu\text{g m}^{-3}$ .

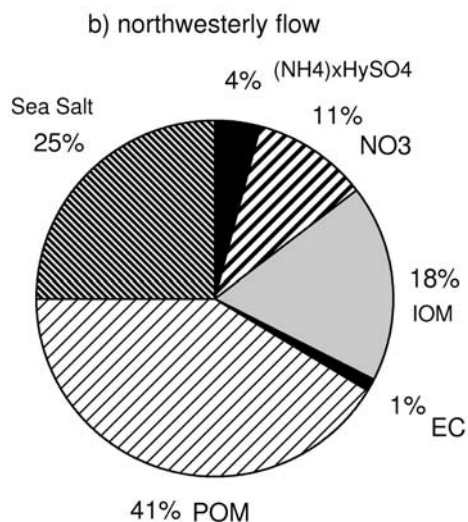


**Figure 5b.** Mass fractions of dominant supermicron chemical components during northwesterly flow. The average gravimetric mass at 55% RH was  $4.7 \pm 1.8 \mu\text{g m}^{-3}$ .

Canada, *McInnes et al.* [1998] concluded that the scattering contribution of organic carbon during conditions of southwesterly flow was at least as much as sulfate aerosol. *Hegg et al.* [1997], based on samples taken off the coast of Virginia during TARFOX in July 1996, concluded that the majority of the dry aerosol light scattering was due to carbonaceous aerosol. Under dry conditions the mean carbonaceous scattering fraction during TARFOX was  $0.66 \pm 0.16$  [*Hegg et al.*, 1997].

[48] It is difficult to extrapolate the component scattering to ambient humidity. A major uncertainty in this analysis is the humidity dependence of scattering of the organic aerosol

(assumed here to be zero) and the humidity dependence of scattering of the internally mixed organic/sulfate aerosol. As the AMS NR POM contained oxidized organic carbon (the average fraction of organic mass due to dicarboxylic acids at  $m/z = 44$  was approximately 12%), the POM component would likely include some water at 55% RH. On the other hand, POM deposited on the surface of particles also may inhibit water uptake by sulfate. Measurements are needed to assess  $f(\text{RH})$  as a function of POM mass fraction, organic composition, acidity and the aerosol mixing state.

### 3.4. Aerosol Light Scattering During Pollution Episodes

[49] Visibility impairment and the potential health effects due to high aerosol concentrations are of particular concern during the elevated pollution episodes that occur along the East Coast of the United States during the summer. While the impactor data collected during NEAQS 2002 were useful for identifying and quantifying the two major regional aerosol components (submicrometer POM and  $(\text{NH}_4)_x\text{H}_y\text{SO}_4$  and associated  $\text{H}_2\text{O}$ ) and in verifying that the submicrometer aerosol dominated aerosol light scattering, the data frequency were not sufficient to capture the smaller space and time scale variations in aerosol concentrations and light scattering. The AMS, however, did measure the two dominant submicrometer aerosol components at a time resolution (two minutes) comparable with the nephelometer measurement of light scattering (one minute). Here we examine two such episodes encountered during NEAQS 2002 (Figure 7). The critical question here is “What were the dominant aerosol species during the haze episodes?”

#### 3.4.1. Case Study 1 (July 22–23)

[50] The highest ozone mixing ratios measured aboard *Ronald H. Brown* during NEAQS 2002 occurred on July 23 (DOY 204) with values reaching nearly 120 ppb (Figure 8).

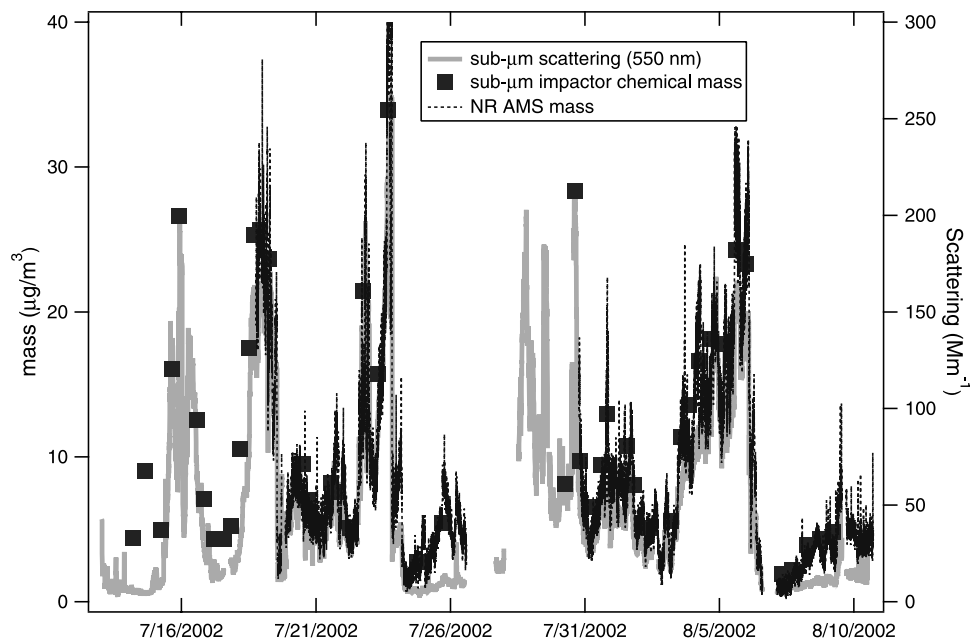


**Figure 6.** Time series of submicrometer scattering (550 nm), total NR AMS mass, and submicrometer impactor chemically analyzed mass.

**Table 2.** Calculated MSE for Submicrometer Aerosol at 55% RH Using Mie Theory and DMPS/APS and AMS Size Distributions<sup>a</sup>

	SW	NW	SW	NW
	POM		(NH <sub>4</sub> ) <sub>x</sub> H <sub>y</sub> SO <sub>4</sub> -H <sub>2</sub> O	
Mie theory – DMPS/APS	5.0 ± 0.35	3.6 ± 0.70	4.0 ± 0.41	2.9 ± 0.95
Mie theory – AMS	5.4 ± 0.40	4.0 ± 0.83	4.6 ± 0.22	3.2 ± 0.95

<sup>a</sup>Units are in m<sup>2</sup> g<sup>-1</sup>. Values given are regional means ± 1 σ standard deviation.

The episode began with a wind shift to southwesterly at about 18Z on 21 July and continued with southwesterly flow until it was terminated abruptly by the passage of a cold front with thunderstorms in the afternoon of July 23 [Angevine *et al.*, 2004]. During this period the ship made cross-wind transects northeast of Cape Ann (Figure 7) in the stable boundary layer. Back trajectories calculated from a wind profiler network showed that the air sampled at the ship had come along the New York City/Boston urban corridor during the previous 24 hours. Transit times from Boston to the ship were approximately 2–3 hours throughout the episode, and transit times from the New York City area were approximately 12 hours [Angevine *et al.*, 2004].

[51] NR POM and NR (NH<sub>4</sub>)<sub>x</sub>H<sub>y</sub>SO<sub>4</sub> concentrations increased during the afternoons (local time) in step with ozone mixing ratios (Figure 8). During the afternoon of July 22, the nss(NH<sub>4</sub>)<sub>x</sub>H<sub>y</sub>SO<sub>4</sub> and aerosol light scattering measurements showed 4 peaks as the ship transited back and forth through power plant plumes (Figure 8). Mie calcu-

lations using the AMS mass size distributions during this period (July 22–23) suggest that POM accounted for 60 ± 6% of σ<sub>sp</sub> (measured at 55% RH).

### 3.4.2. Case Study 2 (August 4–5)

[52] The ship transited in a plume of warm, hazy, polluted air northeast of Cape Ann on August 4 and 5 (Figure 7). On August 4 the ship sailed in a triangle pattern off the coast of New Hampshire. On August 5 the ship made cross wind transects closer to Cape Ann. A stalled frontal trough along the coast led to weak and variable winds at the location of the ship, in sharp contrast to the higher wind speeds (10 m/s) experienced during case study 1. Winds at the beginning of case study 2 were generally from the west, shifting to the south to southwest around 1800Z on August 4 and then back to the west around 2100Z on August 5. Back trajectories show transport from Boston and vicinity to the ship after 1800Z on August 4.

[53] NR POM concentrations were appreciably higher than NR (NH<sub>4</sub>)<sub>x</sub>H<sub>y</sub>SO<sub>4</sub> concentrations during the afternoon (local time) of August 4 when ozone mixing ratios and

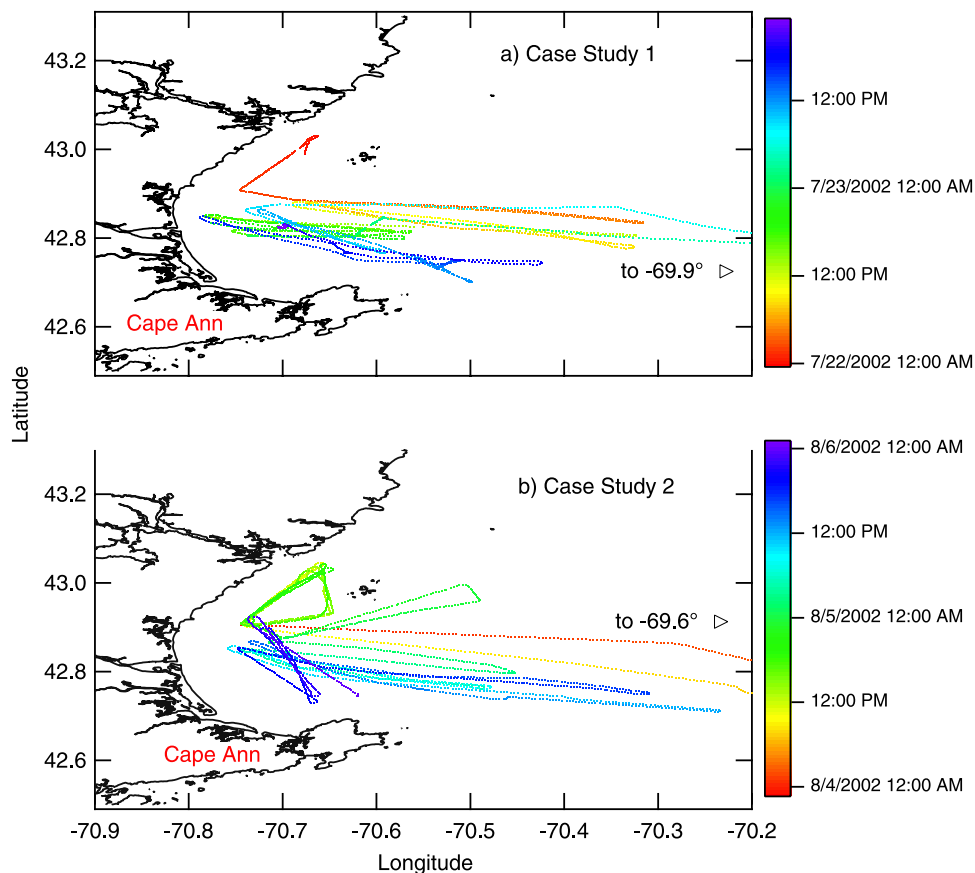


**Figure 7.** (top) Case study 1. July 22 and 23, 2002. (bottom) Case study 2. August 4 and 5, 2002.

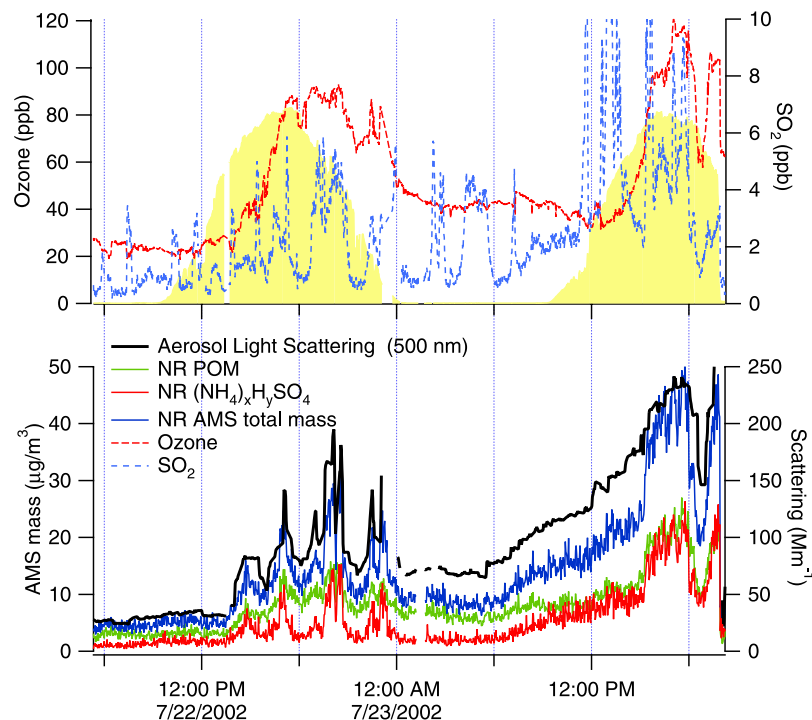


**Figure 8.** Case study 1. (top) SO<sub>2</sub> and O<sub>3</sub> measurements during the case study. Solar insolation is given in the solid yellow. (bottom) AMS mass and measured aerosol light scattering.

aerosol light scattering values were at their peak (Figure 9). NR (NH<sub>4</sub>)<sub>x</sub>H<sub>y</sub>SO<sub>4</sub> concentrations were higher than NR POM concentrations during the morning hours (local time) of August 5. Mie calculations using the AMS mass size distributions during this period suggest that POM accounted for  $57 \pm 11\%$  of  $\sigma_{sp}$  (measured at 55% RH). During both case studies of the high pollution events

sampled during NEAQS 2002, POM dominated aerosol light scattering.

#### 4. Conclusions

[54] Organic aerosols were a dominant component of the total submicrometer aerosol mass and light scattering in the

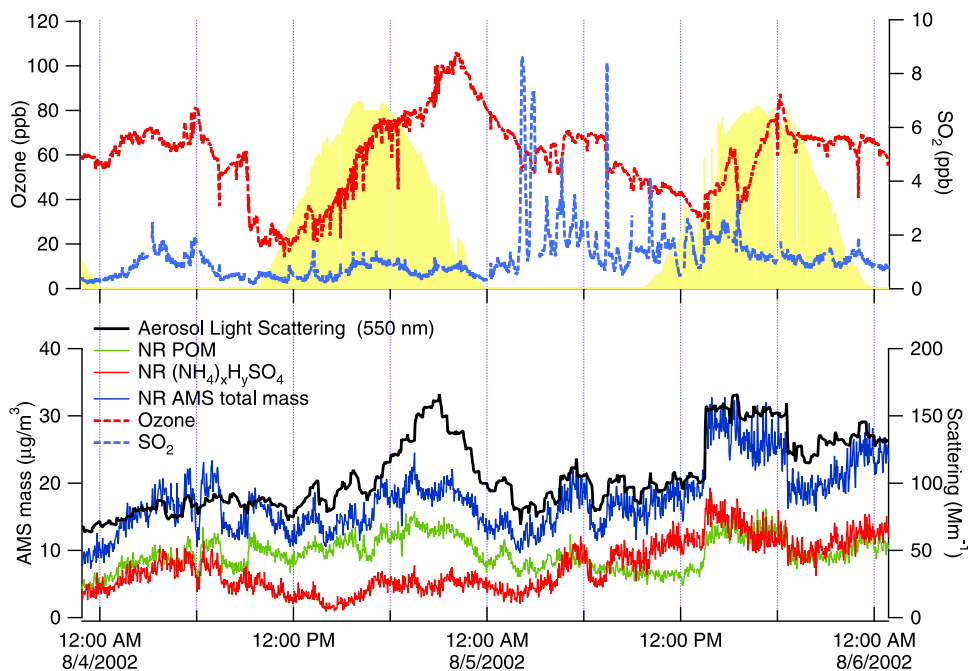


**Figure 9.** Case study 2. (top) SO<sub>2</sub> and O<sub>3</sub> measurements during the case study. Solar insolation is given in the solid yellow. (bottom) AMS mass and measured aerosol light scattering.

marine boundary layer off the New England coast during the summer of 2002. The data are consistent with chemical measurements made at the IMPROVE coastal New England sites during this time period. Ongoing measurements at IMPROVE and AIRMAP stations near the coast and the shipboard measurements during NEAQS 2004 will provide data to determine whether this large organic mass fraction is becoming the norm or was simply an anomaly for this period. Airborne measurements made during NEAQS 2004 will provide data needed to ascertain the importance of organic aerosols in the overlying free troposphere. In the summer, the Gulf of Maine's cold water relative to the warm air creates a shallow stable marine boundary layer [Angevine *et al.*, 2004]. The results reported here thus may be applicable only to this shallow boundary layer.

[55] The aerosol light scattering results reported here are for a humidity of 55% RH, much lower than the average ambient RH measured on the ship ( $79 \pm 13\%$  RH). Further  $f(\text{RH})$  measurements are needed on faster time scales to better capture the relationship between hygroscopic growth, RH, aerosol acidity and the POM mass fraction. Experiments also are needed to determine the water uptake of the POM fraction. This will require a better understanding of the POM composition. In addition, experiments are needed to determine the effect of RH on the aerosol within the AMS.

[56] The reduction in sulfate aerosol concentrations across the United States [Malm *et al.*, 2002] during the past decade may eventually lead to the dominance of organic aerosol over larger areas of the northeastern United States. The NR POM during NEAQS2002 was attributed to secondary anthropogenic processes [de Gouw *et al.*, 2005]. Measurements are now needed to characterize the source and composition of this organic aerosol to determine its health and radiative (e.g., water uptake, cloud nucleating properties) impacts and to develop mitigation strategies if needed.

[57] **Acknowledgments.** We thank the officers and crew of NOAA R/V *Ronald H. Brown* for their cooperation and enthusiasm and T. Miller, D. Hamilton, D. R. Worsnop, M. R. Canagaratna, and B. M. Matthew for technical support. We thank W. Angevine for meteorological support and J. Meagher, F. Fehsenfeld, and D. Albritton for programmatic support. We also thank G. Allen and the NESCAUM team for their review of this manuscript. This research was funded by the Atmospheric Constituents Project of the NOAA Climate and Global Change Program, the NOAA Office of Oceanic and Atmospheric Research, the NOAA Health of the Atmosphere Program, and the New England Air Quality Study. This publication was partially funded by the Joint Institute for the Study of the Atmosphere and Ocean (JISAO) under NOAA cooperative agreement NA17RJ1232, contribution 1104. This is NOAA/PMEL contribution 2774.

## References

- Allan, J. D., J. L. Jimenez, P. I. Williams, M. R. Alfarra, K. N. Bower, J. T. Jayne, H. Coe, and D. R. Worsnop (2003), Quantitative sampling using an Aerodyne aerosol mass spectrometer: 1. Techniques of data interpretation and error analysis, *J. Geophys. Res.*, *108*(D3), 4090, doi:10.1029/2002JD002358.
- Anderson, T. L., and J. A. Ogren (1998), Determining aerosol radiative properties using the TSI 3563 integrating nephelometer, *Aerosol Sci. Technol.*, *29*, 57–69.
- Andreae, M. O. (1983), Soot carbon and excess fine potassium: Long-range transport of combustion-derived aerosols, *Science*, *220*, 1148–1151.
- Angevine, W. M., C. J. Senff, A. B. White, E. J. Williams, J. Koerner, S. T. K. Miller, R. Talbot, P. E. Johnston, S. A. McKeen, and T. Downs (2004), Coastal boundary layer influence on pollutant transport in New England, *J. Appl. Meteorol.*, *43*, 1425–1437.
- Bates, T. S., D. J. Coffman, D. S. Covert, and P. K. Quinn (2002), Regional marine boundary layer aerosol size distributions in the Indian, Atlantic, and Pacific Oceans: A comparison of INDOEX measurements with ACE-1, ACE-2, and Aerosols99, *J. Geophys. Res.*, *107*(D18), 8026, doi:10.1029/2001JD001174.
- Berner, A., C. Lurzer, F. Pohl, O. Preining, and P. Wagner (1979), The size distribution of the urban aerosol in Vienna, *Sci. Total Environ.*, *13*, 245–261.
- Boucher, O., and T. L. Anderson (1995), General circulation model assessment of the sensitivity of direct climate forcing by anthropogenic sulfate aerosols to aerosol size and chemistry, *J. Geophys. Res.*, *100*, 26,117–26,134.
- Brown, S. S., et al. (2004), Nighttime removal of  $\text{NO}_x$  in the summer marine boundary layer, *Geophys. Res. Lett.*, *31*, L07108, doi:10.1029/2004GL019412.
- Cahill, T. A., R. A. Eldred, and P. J. Feeney (1986), Particulate monitoring and data analysis for the National Park Service, 1982–1985, Univ. of Calif., Davis.
- Carrico, C. M., P. Kus, M. J. Rood, P. K. Quinn, and T. S. Bates (2003), Mixtures of pollution, dust, sea salt, and volcanic aerosol during ACE-Asia: Light scattering properties as a function of relative humidity, *J. Geophys. Res.*, *108*(D23), 8650, doi:10.1029/2003JD003405.
- Charlson, R. J., T. L. Anderson, and H. Rodhe (1999), Direct climate forcing by anthropogenic aerosols: Quantifying the link between atmospheric sulfate and radiation, *Contrib. Atmos. Phys.*, *72*, 79–94.
- Cheng, Y. S., B. T. Chen, H. C. Yeh, I. A. Marshall, J. P. Mitchell, and W. D. Griffiths (1993), Behavior of compact nonspherical particles in the TSI aerodynamic particle sizer model APS33B: Ultra-Stokesian drag forces, *Aerosol Sci. Technol.*, *19*, 255–267.
- de Gouw, J. A., et al. (2005), Budget of organic carbon in a polluted atmosphere: Results from the New England Air Quality Study in 2002, *J. Geophys. Res.*, *110*, D16305, doi:10.1029/2004JD005623.
- Draxler, R. R. (1992), Hybrid Single-Particle Lagrangian Integrated Trajectories (HY-SPLIT): Version 3.0—User's guide and model description, *Tech. Rep. ERL ARL-195*, Natl. Oceanic and Atmos. Admin., Silver Spring, Md. (Available at <http://www.arl.noaa.gov/ready/hysplit4.html>)
- Driscoll, C. T., et al. (2003), Nitrogen pollution in the Northeastern United States: Sources, effects, and management options, *BioScience*, *53*, 357–374.
- Feely, R. A., G. J. Massoth, and G. T. Lebon (1991), Sampling of marine particulate matter and analysis by X-ray fluorescence spectrometry, in *Marine Particles: Analysis and Characterization*, *Geophys. Monogr. Ser.*, vol. 63, edited by D. C. Hurd and D. W. Spencer, pp. 251–257, AGU, Washington, D. C.
- Guenther, A., et al. (1995), A global model of natural volatile organic compound emissions, *J. Geophys. Res.*, *100*, 8873–8892.
- Guenther, A., C. Geron, T. Pierce, B. Lamb, P. Harley, and R. Fall (2000), Natural emissions of non-methane volatile organic compounds, carbon monoxide, and oxides of nitrogen from North America, *Atmos. Environ.*, *34*, 2205–2230.
- Harrison, R. M., and J. Yin (2000), Particulate matter in the atmosphere: Which particle properties are important for its effects on health?, *Sci. Tot. Environ.*, *249*, 85–101.
- Hegg, D. A., et al. (1997), Chemical apportionment of aerosol column optical depth off the mid-Atlantic coast of the United States, *J. Geophys. Res.*, *102*, 25,293–25,303.
- Holland, H. D. (1978), *The Chemistry of the Atmosphere and Oceans*, p. 154, John Wiley, Hoboken, N. J.
- Intergovernmental Panel on Climate Change (IPCC) (2001), *Climate Change 2001: The Scientific Basis*, edited by J. T. Houghton et al., 896 pp., Cambridge Univ. Press, New York.
- Jayne, J. T., D. C. Leard, X. Zhang, P. Davidovits, K. A. Smith, C. E. Kolb, and D. R. Worsnop (2000), Development of an aerosol mass spectrometer for size and composition analysis of submicron particles, *Aerosol Sci. Technol.*, *33*, 49–70.
- Mader, B. T., et al. (2003), Sampling methods used for the collection of particle-phase organic and elemental carbon during ACE-Asia, *Atmos. Environ.*, *37*(11), 1435–1449.
- Malm, W. C., J. F. Sisler, D. Huffman, R. A. Eldred, and T. A. Cahill (1994), Spatial and seasonal trends in particle concentration and optical extinction in the United States, *J. Geophys. Res.*, *99*, 1347–1370.
- Malm, W. C., B. A. Schichtel, R. B. Ames, and K. A. Gebhart (2002), A 10-year spatial and temporal trend of sulfate across the United States, *J. Geophys. Res.*, *107*(D22), 4627, doi:10.1029/2002JD002107.
- Malm, W. C., B. A. Schichtel, M. L. Pitchford, L. L. Ashbaugh, and R. A. Eldred (2004), Spatial and monthly trends in speciated fine particle concentration in the United States, *J. Geophys. Res.*, *109*, D03306, doi:10.1029/2003JD003739.

- McInnes, L., M. Bergin, J. Ogren, and S. Schwartz (1998), Apportionment of light scattering and hygroscopic growth to aerosol composition, *Geophys. Res. Lett.*, *25*, 513–516.
- Miller, S. T. K., and B. D. Keim (2003), Synoptic-scale controls on the sea breeze of the central New England coast, *Weather Forecasting*, *18*, 236–248.
- NARSTO (2003), Particulate matter science for policy makers, a NARSTO assessment, NARSTO Manage. Off. (Envair), Pasco, Wash., Feb. (Available at <http://www.cgenv.com/Narsto/>)
- Novakov, T., D. A. Hegg, and P. V. Hobbs (1997), Airborne measurements of carbonaceous aerosols on the east coast of the United States, *J. Geophys. Res.*, *102*, 30,023–30,030.
- Quimette, J. R., and R. C. Flagan (1982), The extinction coefficient of multicomponent aerosols, *Atmos. Environ.*, *16*, 2405–2419.
- Perry, K. D., T. A. Cahill, R. A. Eldred, D. D. Dutcher, and T. E. Gill (1997), Long-range transport of North African dust to the eastern United States, *J. Geophys. Res.*, *102*, 11,225–11,238.
- Putaud, J. P., et al. (2000), Chemical mass closure and assessment of the origin of the submicron aerosol in the marine boundary layer and the free troposphere at Tenerife during ACE-2, *Tellus, Ser. B*, *52*, 141–168.
- Quinn, P. K., and T. S. Bates (2003), North American, Asian, and Indian haze: Similar regional impacts on climate?, *Geophys. Res. Lett.*, *30*(11), 1555, doi:10.1029/2003GL016934.
- Quinn, P. K., and T. S. Bates (2005), Regional aerosol properties: Comparisons of boundary layer measurements from ACE 1, ACE 2, Aerosols99, INDOEX, ACE Asia, TARFOX, and NEAQS, *J. Geophys. Res.*, *110*, D14202, doi:10.1029/2004JD004755.
- Quinn, P. K., and D. J. Coffman (1998), Local closure during ACE 1: Aerosol mass concentration and scattering and backscattering coefficients, *J. Geophys. Res.*, *103*, 16,575–16,596.
- Quinn, P. K., D. J. Coffman, V. N. Kapustin, T. S. Bates, and D. S. Covert (1998), Aerosol optical properties in the marine boundary layer during ACE 1 and the underlying chemical and physical aerosol properties, *J. Geophys. Res.*, *103*, 16,547–16,563.
- Quinn, P. K., D. J. Coffman, T. S. Bates, T. L. Miller, J. E. Johnson, E. J. Welton, C. Neusüss, M. Miller, and P. Sheridan (2002), Aerosol optical properties during INDOEX 1999: Means, variabilities, and controlling factors, *J. Geophys. Res.*, *107*(D19), 8020, doi:10.1029/2000JD000037.
- Savoie, D. L., and J. M. Prospero (1980), Water-soluble potassium, calcium, and magnesium in the aerosols over the tropical North Atlantic, *J. Geophys. Res.*, *85*, 385–392.
- Schauer, J. J., et al. (2002), ACE Asia intercomparison of a thermal-optical method for the determination of particle-phase organic and elemental carbon, *Environ. Sci. Technol.*, *37*, 993–1001, doi:10.1021/es020622f.
- Schindler, D. W., S. E. M. Kasian, and R. H. Hesslein (1989), Biological impoverishment in lakes of the Midwestern and Northeastern United States from acid rain, *Environ. Sci. Technol.*, *23*, 573–580.
- Turpin, B. J., and H. Lim (2001), Species contribution to PM<sub>2.5</sub> concentrations: Revisiting common assumptions for estimating organic mass, *Aerosol Sci. Technol.*, *35*, 602–610.
- United States Environmental Protection Agency (2003a), Latest findings on national air quality, 2002 status and trends, *EPA Publ.*, *454/K-03-001*.
- United States Environmental Protection Agency (2003b), National air quality and emissions trends report, 2003 special studies edition, *EPA Publ.*, *454/R-03-005*.
- Wang, H. C., and W. John (1987), Particle density correction for the aerodynamic particle sizer, *Aerosol Sci. Technol.*, *6*, 191–198.
- White, W. H. (1986), On the theoretical and empirical basis for apportioning extinction by aerosols: A critical review, *Atmos. Environ.*, *20*, 1659–1672.

---

T. S. Bates, D. J. Coffman, J. E. Johnson, and P. K. Quinn, Pacific Marine Environmental Laboratory, NOAA, 7600 Sand Point Way N.E., Seattle, WA 98115, USA. (tim.bates@noaa.gov)

A. M. Middlebrook, Aeronomy Laboratory, NOAA, 325 Broadway, Boulder, CO 80303, USA.